

## Rapid Communications

*The Rapid Communications section is intended for the accelerated publication of important new results. Since manuscripts submitted to this section are given priority treatment both in the editorial office and in production, authors should explain in their submittal letter why the work justifies this special handling. A Rapid Communication should be no longer than 3½ printed pages and must be accompanied by an abstract. Page proofs are sent to authors, but, because of the accelerated schedule, publication is not delayed for receipt of corrections unless requested by the author or noted by the editor.*

### Depth profiling of elastic strains in lattice-mismatched semiconductor heterostructures and strained-layer superlattices

D. J. Olego, K. Shahzad,\* J. Petruzzello, and D. Cammack

*Philips Laboratories, North American Philips Corporation, Briarcliff Manor, New York 10510*

(Received 10 August 1987)

The elastic strains in regions near the top surface of strained-layer structures can be quite different from those in deeper portions of the samples. This effect has been established in epitaxial layers of ZnSe grown on GaAs and ZnSe-ZnS<sub>x</sub>Se<sub>1-x</sub> strained-layer superlattices. The depth dependence of the strains was determined with Raman scattering measurements performed under laser excitation below and above the band gap. The strain values near the top surface are driven by a stronger relaxation of the in-plane lattice constants towards equilibrium. This relaxation appears to be independent of the generation of misfit dislocations.

The epitaxial growth of lattice-mismatched semiconductors provides an extra degree of freedom in tailoring optical and transport properties of semiconductor heterostructures and superlattices.<sup>1</sup> The ability to modify these properties has impacted the fundamental and applied fields of semiconductor research. The lattice mismatch between epitaxial layers and substrates in heterostructures or between thin layers in superlattices can be as large as a few percent and therefore considerable elastic strains are usually present in the grown layers. The strains influence the growth habits of the epitaxial layers and play a major role in determining the final values of parameters such as forbidden gaps, band offsets, and carrier mobilities.<sup>1,2</sup> That is why the characterization of the state of strain and its dependence on sample parameters is an important issue in strained-layer epitaxy. Though a considerable amount of experimental work has been carried out to this effect, there is one aspect of the strain behavior that has not been dealt with in great detail up to now. This is the question of whether the strains are constant throughout the strained-layer structures or if some relaxation does take place and different strain values are possible as a function of depth into the sample. Answers to this question will help to understand the nature of the congruent to free-standing transition. The possibility of inhomogeneous strains is expected to impact the analysis of optical measurements such as excitation and modulation spectroscopies and resonant Raman scattering. It will also play a role in the experimental search for the novel nonlinear optical properties which have been recently predicted in strained-layer superlattices.<sup>3</sup>

In this paper we report on strain variations within a sample found in two strained systems: ZnSe epitaxial lay-

ers grown on GaAs substrates and superlattices of ZnSe-ZnS<sub>x</sub>Se<sub>1-x</sub>. In both systems the strain values for regions of the samples near the top surface are different from those determined by averaging through the entire specimen. The strains near the top surface are influenced by a stronger relaxation of the lattice constant towards the equilibrium values. In the case of the superlattices this implies more strain in the individual ZnSe layers at the top and a gradual transition to the free-standing state. The strains were determined by measuring with Raman scattering the shifts in the frequencies of the long-wavelength optical phonons.<sup>4</sup> The depth profiling is achieved by changing the wavelength of the incoming photons and therefore varying the skin depth from which the Raman signal originates. In addition to the investigation of the strains at different depths into the samples, we also studied the relaxation of the strains in the ZnSe layers of the ZnSe-GaAs heterostructure as a function of the ZnSe thickness and compared the strain values obtained with Raman scattering to those determined with photoluminescence, x-ray diffraction, and transmission electron microscopy techniques.<sup>5,6</sup> Good agreement is found between Raman and the other techniques for the strain values representing averages throughout the entire layers.

The samples used in this investigation were grown by molecular-beam epitaxy on (100) GaAs substrates. The details of the growth were described in previous publications.<sup>5,7</sup> The thickness  $D$  of the ZnSe layers in the heterostructures ranges between 50 and 1000 nm. We present data for a superlattice sample consisting of alternating layers of 5.5 nm of ZnSe and 6 nm of ZnS<sub>0.19</sub>Se<sub>0.81</sub> grown on a 1000-nm-thick ZnSe buffer layer. The total superlattice thickness is 4300 nm. The Raman scattering mea-

measurements were performed in backscattering geometry with the sample mounted in a cold finger of a closed-cycle cryostat. The sample temperature during the measurements was 12 K. The Raman spectra were excited either with the 488-nm line of an Ar<sup>+</sup>-ion laser or the 413.1-nm line of a Kr<sup>+</sup>-ion laser. The ZnSe and ZnS<sub>0.19</sub>Se<sub>0.81</sub> layers are transparent to the 488-nm incoming radiation,<sup>8</sup> and the Raman light yields information about regions of the samples away from the top surface. The 413.1-nm photons are absorbed in a skin depth of  $\approx 100$  nm and therefore the Raman light will sample  $\approx 50$  nm from the top surface down.<sup>8,9</sup> The selection rules for the scattering process allow only the creation of the near zone center longitudinal optical (LO) phonons.<sup>9</sup>

We discuss first the results on the ZnSe epitaxial layers grown on GaAs. Figure 1 shows the Stokes-Raman spectra due to the LO phonons of a  $\approx 180$ -nm-thick ZnSe layer taken with the two laser wavelengths used in this experiment. The Raman peaks are blue shifted with respect to the LO phonon frequency of bulk ZnSe at  $256.3 \text{ cm}^{-1}$  which is indicated by the arrow. The shift is larger for the spectrum excited with below band gap light at 488 nm. Similar trends in the shifts are observed for ZnSe films of other thicknesses  $D$ . However, the absolute values of the shifts become smaller with increasing  $D$ . The shifts of the LO peaks to higher energies arise from in-plane compressive strains in the ZnSe layers due to the lattice mismatch with the GaAs substrate as discussed below. The undisturbed LO frequency was determined very accurately by measurements done in bulk ZnSe wafers with (100) and (111) surfaces as well as in ZnSe epitaxial layers grown on ZnSe substrates. In these cases no dependence of the LO peak positions was found on the exciting laser wavelength.

The lattice constant of ZnSe (0.5669 nm) is slightly larger than that of GaAs (0.5654 nm). Hence the epitaxial growth of ZnSe on (100) GaAs surfaces will produce a biaxial compression of the unit cell of ZnSe along the  $x$

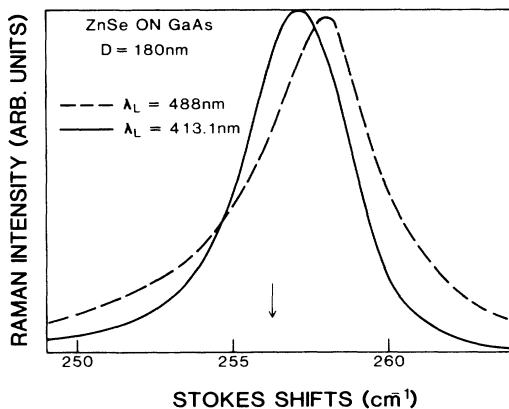


FIG. 1. Raman spectra due to longitudinal optical phonons of a ZnSe layer grown on GaAs. The Raman lines are shifted to higher frequencies with respect to the bulk longitudinal optical frequency indicated by the arrow. The shifts arise because compressive strains are present in the layer. The strain values change throughout the sample.

and  $y$  directions parallel to the grown surface. The nonzero components of the strain tensor are  $\epsilon_{xx} = \epsilon_{yy} = \epsilon = (a_{\parallel} - a_{\text{ZnSe}})/a_{\text{ZnSe}}$  and  $\epsilon_{zz} = 2S_{12}(S_{11} + S_{12})^{-1}\epsilon$ . The bulk value of the ZnSe lattice constant is represented by  $a_{\text{ZnSe}}$  and  $a_{\parallel}$  gives the in-plane value along the  $(x, y)$  directions in the epitaxial layers.  $S_{ij}$  are the elastic compliance constants of ZnSe. For compressive strains  $\epsilon$  is negative in the convention adopted here. Under these conditions the LO phonon frequency  $\omega$  depends on  $\epsilon$  according to the following expression:<sup>4</sup>

$$\omega = \omega_0 + 2\Delta\Omega_H - \frac{2}{3}\Delta\Omega, \quad (1)$$

where  $\omega_0$  is the undisturbed bulk frequency and  $\Delta\Omega_H$  and  $\Delta\Omega$  are given respectively by

$$\Delta\Omega_H = \frac{p+2q}{6\omega_0^2} \left( \frac{S_{11}+2S_{12}}{S_{11}+S_{12}} \right) \omega_0\epsilon, \quad (2)$$

and

$$\Delta\Omega = \frac{p-q}{2\omega_0^2} \left( \frac{S_{11}-S_{12}}{S_{11}+S_{12}} \right) \omega_0\epsilon. \quad (3)$$

For ZnSe the deformation potentials  $-(p+2q)/6\omega_0^2$  and  $(p-q)/2\omega_0^2$  are 0.9 and 0.62, respectively.<sup>4,10</sup> We take  $S_{11}+S_{12}=0.0145$ ,  $S_{11}+2S_{12}=0.006$ , and  $S_{11}-S_{12}=0.0315$  in  $\text{GPa}^{-1}$  and replace the numerical values in Eqs. (1–3) to obtain the simple relationship

$$\omega = 256.3 - 421.14\epsilon, \quad (4)$$

with  $\omega$  in units of  $\text{cm}^{-1}$ . Equation (4) predicts blue shifts in  $\omega$  for negative  $\epsilon$ , as observed experimentally. Furthermore, the smaller shift observed in Fig. 1 for the 413.1-nm case can be explained in terms of a reduced  $\epsilon$  near the top surface of the layer as compared with the  $\epsilon$  value representative of regions of the sample closer to the interface with the substrate (488-nm excitation). Quantitative estimates of  $\epsilon$  were obtained by replacing  $\omega$  in Eq. (4) with the measured Raman frequencies and the results are plotted in Fig. 2. Smaller values of  $\epsilon$  near the top are encountered for layers of different  $D$  which points out that we are dealing with a universal behavior of the system and not with a property of a particular sample.

The data in Fig. 2 point out a related aspect of strain release. In addition to the relaxation of  $\epsilon$  moving away from the interface with the substrate, there is also a decrease in  $\epsilon$  with increasing  $D$ . This effect was studied before with photoluminescence (PL), x-ray diffraction, and transmission electron microscopy (TEM).<sup>5,6</sup> Therefore, it seems appropriate to compare the Raman data with the results of Refs. 5 and 6 and, for this purpose, we have incorporated them in Fig. 2. A good agreement is found between the 488-nm Raman data (sampling the entire layers) and these other determinations of  $\epsilon$ . For the range of  $D$  studied here, PL and x-ray experiments also yield values of  $\epsilon$  which are averages throughout the layers. The PL light can originate inside the samples at depths on the order of the diffusion lengths of the photoexcited electrons and holes. For molecular beam epitaxy grown layers, diffusion lengths of 1000 nm are not unusual. On the other hand, the attenuation length of the x rays is much larger than  $D$  and the entire samples are illuminated by the x rays. Finally, the TEM determinations are partially

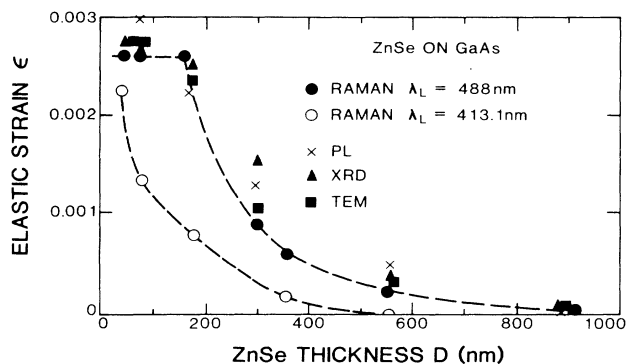


FIG. 2. Dependence of the elastic strains in the ZnSe layers of ZnSe-GaAs heterostructures as a function of layer thickness and depth into the sample. Results from Refs. 5 and 6 included for comparison. The dashed lines were drawn through the Raman data to help the eyes.

based on lattice parameters measured with x-ray diffraction.

The magnitude of  $\epsilon$  for  $D \leq 180$  nm obtained by probing throughout the layers is within experimental uncertainties the expected one for the case in which  $a_{\parallel}$  takes the value of the GaAs lattice constant. This situation corresponds to coherent growth without defects being introduced at the interface between the epitaxial layer and the substrate. The decrease in  $\epsilon$  with  $D$  above 180 nm is associated with the appearance of misfit dislocations at this interface. However, we see in Fig. 2 that the additional release of  $\epsilon$  near the top occurs for films below and above the critical thickness which triggers the misfit dislocation formation. Therefore, we conclude that there is no correlation between this extra relaxation of  $\epsilon$  at the top and the generation of the misfit dislocations. This observation is relevant for the theoretical models trying to describe the microscopic mechanisms for strain relaxation.<sup>2</sup> More experimental and theoretical work is needed to understand if this effect can proceed through the generation of defects other than misfit dislocations that will allow  $a_{\parallel}$  to relax faster to the  $a_{\text{ZnSe}}$  value at the surface. For example, we found that stacking faults are the dominant structural defects in the ZnSe layers below critical layer thickness and are also commonly observed in other congruently grown strained systems.<sup>11</sup>

The stronger relaxation of  $a_{\parallel}$  towards its equilibrium value near the top surface is also present in the ZnSe-ZnS<sub>0.19</sub>Se<sub>0.81</sub> strained-layer superlattice. Figure 3 shows the Stokes-Raman spectra of the superlattice in the optical region of the LO phonons of the ZnSe layers (peaks above 255 cm<sup>-1</sup>) and the LO ZnSe-like modes of the ZnS<sub>0.19</sub>Se<sub>0.81</sub> layers (peaks below 255 cm<sup>-1</sup>). The differences in the relative intensities of the Raman peaks for the two laser wavelengths are related to resonant effects that will be addressed in a separate publication. The arrows in Fig. 3 establish the undisturbed frequencies of the LO phonons of bulk ZnSe and ZnS<sub>0.19</sub>Se<sub>0.81</sub>. The LO peaks of the ZnSe layers appear blue shifted and those of the ZnS<sub>0.19</sub>Se<sub>0.81</sub> ones are red shifted. Contrary to the case of the ZnSe layers in the ZnSe-GaAs hetero-

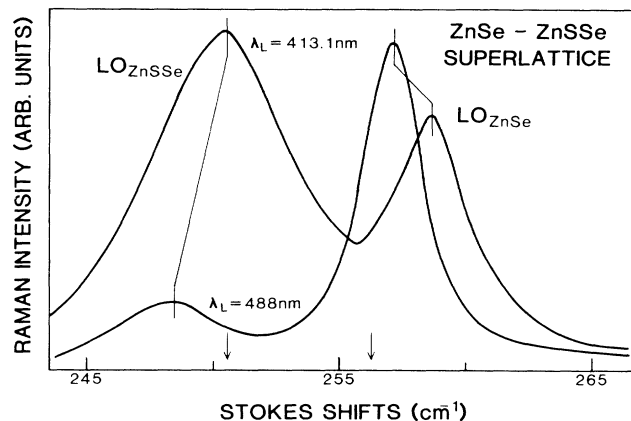


FIG. 3. Raman spectra of a ZnSe-ZnS<sub>0.19</sub>Se<sub>0.81</sub> strained-layer superlattice in the frequency region of the ZnSe-like longitudinal optical phonons. The arrows correspond to the undisturbed bulk frequencies. The dependence of the blue and red shifts on the laser wavelength indicates strain variations as a function of depth.

structures, we see in Fig. 3 that the shifts to higher frequencies of the LO phonons of the ZnSe layers in the superlattice are larger for above band-gap excitation. On the other hand, the red shifts of the LO modes of ZnS<sub>0.19</sub>Se<sub>0.81</sub> are smaller when the Raman light comes from the top region of the sample (413.1 nm laser excitation). The blue and red nature of the shifts is in qualitative agreement with the expectation that the ZnSe layers will be under biaxial compression and the ZnS<sub>0.19</sub>Se<sub>0.81</sub> under biaxial tension. The lattice constant  $a_{\text{ZnS}_{0.19}\text{Se}_{0.81}}$  is  $\approx 0.562$  nm.<sup>8</sup> This value is substantially smaller than  $a_{\text{ZnSe}}$  and an alternating pattern of  $\epsilon$  will be produced in the multilayer structure. We infer from the behavior of the Raman peaks that the strains are not uniform through the superlattice structure and that the magnitude of the compressive (tensile) strains in the ZnSe (ZnS<sub>0.19</sub>Se<sub>0.81</sub>) layers increases (decreases) near the top surface. From the measured shifts in the ZnSe LO frequencies we determined with Eq. (4)  $\epsilon \approx 0.0049$  in the ZnSe layers close to the top surface of the superlattice and 0.002 for an average throughout the sample.

For the total thickness of the superlattice (4300 nm) and the lattice mismatch between the layers one expects the superlattice to be a free standing one,<sup>1,2</sup> in which the equilibrium lattice constant  $a_{\parallel}^0$  along  $x$  and  $y$  is determined by  $\approx a_{\text{ZnSe}} - d_{\text{ZnS}_{0.19}\text{Se}_{0.81}} (d_{\text{ZnS}_{0.19}\text{Se}_{0.81}} + d_{\text{ZnSe}})^{-1} \times (a_{\text{ZnSe}} - a_{\text{ZnS}_{0.19}\text{Se}_{0.81}})$  with  $d_i$  the thickness of the individual layers. For the parameters of our sample  $a_{\parallel}^0$  should be  $\approx 2^{-1}(a_{\text{ZnSe}} + a_{\text{ZnS}_{0.19}\text{Se}_{0.81}}) = 0.5644$  nm and the associated strain in the ZnSe layers  $\epsilon = (a_{\parallel}^0 - a_{\text{ZnSe}})/a_{\text{ZnSe}}$  on the order of 0.0043. This value of  $\epsilon$  is very close to the measured one near the top of the superlattice but differs substantially from the one obtained by probing deeper into the sample. The Raman results together with the comparison between theory and experiment indicate that the transition from the state in which the superlattice conforms to the substrate or buffer layer into the free-standing case is not a sharp one. The smaller  $\epsilon$  in regions

near to the buffer layer (488 nm laser excitation) arises because the superlattice  $a_{\parallel}$  is closer to  $a_{\text{ZnSe}}$  than to  $a_{\parallel}^0$ . Concomitant with the reduced  $\epsilon$  in the ZnSe layers, the biaxial tension in the ternary layers increases as evidenced by the more pronounced red shifts of the Raman peaks. With  $a_{\parallel}$  approaching  $a_{\parallel}^0$  near the top surface the biaxial tension in the  $\text{ZnS}_{0.19}\text{Se}_{0.81}$  layers diminishes and the compression in the ZnSe layers increases. The microscopic mechanism of the relaxation to the free-standing state has to be elucidated. Preliminary TEM investigations of this and similar structures show the characteristic misfit dislocations at the superlattice buffer layer interface. However, it appears that they are not efficient enough to allow for a complete relaxation to the equilibrium state and, as in the case of the epitaxial layers, the role of other defects cannot be disregarded.

In summary, we have shown in the case of two strained-layer systems that the strains are not uniform as a function of depth into the sample. The strains near the top surfaces are determined by a stronger relaxation of the lattice constants towards the equilibrium values. This effect has been seen in samples below and above the critical layer thickness for the creation of misfit dislocations. The transition from congruent to free standing takes place gradually. The possibility that other type of defects play a role in strain relaxation has been suggested but additional experimental and theoretical work is needed in the subject.

The help of R. Dalby in the sample growth is gratefully acknowledged.

\*Formerly called K. Mohammed.

- <sup>1</sup>G. C. Osbourn, IEEE J. Quantum Electron. **QE-22**, 1677 (1986).  
<sup>2</sup>R. People, IEEE J. Quantum Electron. **QE-22**, 1696 (1986), and references therein.  
<sup>3</sup>D. L. Smith and C. Mailhot, Phys. Rev. Lett. **58**, 1264 (1987).  
<sup>4</sup>F. Cerdeira, C. J. Buchenauer, F. H. Pollak, and M. Cardona, Phys. Rev. B **5**, 580 (1972).  
<sup>5</sup>K. Mohammed, D. A. Cammack, R. Dalby, P. Newbury, B. L. Greenberg, J. Petruzzello, and R. Bhargava, Appl. Phys. Lett. **50**, 37 (1987).  
<sup>6</sup>J. Petruzzello, B. L. Greenberg, D. A. Cammack, and R. Dalby (unpublished).  
<sup>7</sup>K. Mohammed, D. J. Olego, P. Newbury, D. A. Cammack,

R. Dalby, and H. Cornelissen, Appl. Phys. Lett. **50**, 1820 (1987).

- <sup>8</sup>H. Hartmann, R. March, and B. Selle, in *Current Topics in Material Science*, edited by E. Kaldis (North-Holland, Amsterdam, 1982), Vol. 9, p. 5, and references therein.  
<sup>9</sup>M. Cardona, in *Light Scattering in Solids II*, edited by M. Cardona and G. Güntherodt (Springer, Heidelberg, 1982), p. 19.  
<sup>10</sup>B. Weinstein and R. Zallen, in *Light Scattering in Solids IV*, edited by M. Cardona and G. Güntherodt (Springer, Heidelberg, 1984), p. 463.  
<sup>11</sup>D. K. Biegelsen, F. A. Ponce, A. J. Smith, and J. C. Tramontana, J. Appl. Phys. **61**, 1856 (1987).